Model for Diffraction Excitation

G. A. Jaroszkiewicz and P. V. Landshoff
Department of Applied Mathematics and Theoretical Physics, University of Cambridge, Cambridge, England
(Received 13 August 1973)

A model in which the Pomeron couples to quarks in a way that resembles the coupling of an SU(3)-scalar photon has previously been shown to be successful for p-p elastic scattering. The analysis is now extended to the inclusive process $pp \to pX$ at small t and missing mass beyond the resonance region. There are no free parameters and agreement with published data is good.

A surprisingly successful picture of high-energy lepton-hadron interactions may be constructed by visualizing the nucleon as being composed of three "valence" quarks, which give it its quantum numbers, together with a neutral infinite "sea" of virtual quark-antiquark pairs.[1] Other hadrons are assigned an analogous structure. With extra dynamical assumptions, this picture has been extended[2,3] to high-energy elastic scattering of pairs of hadrons at small momentum transfer t. In essence, it was supposed that the sea is responsible for generating the Pomeron, and that this couples mainly to the valence quarks through a simple γ^μ coupling (Fig. 1). The effect of this is that at small t the Pomeron couples in a way closely resembling the coupling of an SU(3)-scalar photon, with, of course, important differences associated with signature and charge-conjugation properties.

Although there is no *a priori* reason why such a model for the strong interactions should be valid, it does have three striking successes, each of which emerges as an approximate prediction of the model[2]:

(a) the quark-counting rule for total cross sections (calculated from the imaginary part of the forward elastic amplitude),

(b) s-channel helicity conservation for the coupling of the Pomeron to the nucleon at small t (to obtain this result, one uses as input the fact that the anomalous magnetic moment of the nucleon is almost entirely isovector), and

(c) the correct shape for the high-energy elastic pp differential cross section at small t, including the change of slope at $|t| \approx 0.1$ GeV^2.

If $f^{\mathcal{P}}(t)$ and $f^{\mathfrak{R}}(t)$ are the amplitudes for the emission of $\mathcal{P}$ and $\mathfrak{R}$ valence quarks by the nucleon, the amplitude corresponding to Fig. 1 is[2]

$$-\beta^2[f^{\mathcal{P}}(t)+f^{\mathfrak{R}}(t)]^2\left(\frac{s}{m^2}\right)^{\alpha_P(t)-1}\frac{1+e^{-i\pi\alpha_P(t)}}{\sin\pi\alpha_P(t)} \times \bar{u}(c)\gamma^\mu u(a)\bar{u}(d)\gamma_\mu u(b)\ , \quad (1)$$

where the constant β measures the coupling of the Pomeron to the quarks and we have taken the Regge scale parameter s_0 to be equal to the square of the nucleon mass, m. The Dirac form factors of the proton and neutron are

$$F_1^p(t) = \tfrac{2}{3}f^{\mathcal{P}}(t) - \tfrac{1}{3}f^{\mathfrak{R}}(t)\ ,$$
$$F_1^n(t) = \tfrac{2}{3}f^{\mathfrak{R}}(t) - \tfrac{1}{3}f^{\mathcal{P}}(t)\ , \quad (2)$$

so that if we take $F_1^n(t) = 0$,

$$f^{\mathfrak{R}}(t) = \tfrac{1}{2}f^{\mathcal{P}}(t) = F_1^p(t)\ . \quad (3)$$

Thus the unpolarized elastic pp differential cross section is

$$\frac{d\sigma}{dt} = \frac{[3\beta F_1^p(t)]^4}{4\pi\sin^2[\frac{1}{2}\pi\alpha_P(t)]}\left(\frac{s}{m^2}\right)^{2\alpha_P(t)-2}\ . \quad (4)$$

From the experimental data,[4] $d\sigma/dt \approx 80$ mb/GeV^2 at $t=0$, so that

$$\frac{\beta^4}{4\pi} \approx 1.0 \text{ mb/GeV}^2\ . \quad (5)$$

Throughout this paper we shall ignore the small change[4] of $d\sigma/dt$ at $t=0$ with energy; that is, we suppose that the Pomeron is a simple pole.

We use the dipole form for $G_M(t) \approx \mu G_E(t)$:

$$F_1^p(t) = \frac{4m^2 - 2.79t}{4m^2 - t}\,\frac{1}{(1-t/0.71)^2}\ . \quad (6)$$

We take a linear Pomeron trajectory and determine its slope from the requirement that (4) gives the correct exponential slopes for $d\sigma/dt$. This gives $\alpha_P' = 0.25 \pm 0.02$ GeV^{-2}; that is,

$$\alpha_P(t) = 1 + \tfrac{1}{4}t\ . \quad (7)$$

The change of slope[5] at $|t| \approx 0.1$ is then reproduced. In Table I we compare the calculated values of the exponential slope to either side of this break with the experimental values,[5] and in Fig. 2 we plot the calculated curve for $d\sigma/dt$ together with the unnormalized data. The expression (4) fits the data in the range $460 \leq s \leq 2800$ GeV^2. Note that if the required Pomeron slope had been larger this would

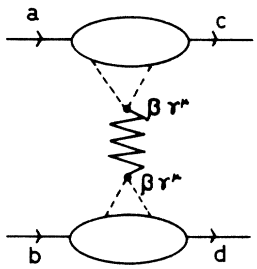

FIG. 1. Diagram for elastic pp scattering.

have restricted the expected range of values of t for which the model could be valid; the Pomeron can resemble an SU(3)-scalar photon only when its "spin" $\alpha_P(t)$ is close to unity.

In this paper we extend the model to inelastic diffractive processes, $pp \to pX$, in which a system X of missing mass M is produced at small t. Ravndal[3] has considered the case where M is in the resonance region. Here we concentrate on values of M which are larger, but sufficiently low for the predominant exchange of Fig. 3 to be that of the Pomeron. By considering recent data[6] we estimate that this requires s/M^2 greater than about 10 or 20. Also, for the reason we have given above, we restrict $|t|$ to values less than about 0.5 GeV^2; in this respect our attitude contrasts with that of Berman and Jacob,[7] who have applied a related model at large t.

The contribution from Fig. 3 is calculated by methods that have been described elsewhere.[8] The result involves the electroproduction structure functions $W_1(\nu, q^2)$ and $W_2(\nu, q^2)$ for a proton target,[9] where

$$q^2 = -t, \qquad 2m\nu = M^2 + q^2 - m^2 . \tag{8}$$

We decompose these functions into sums of contributions from the different types of quarks to which

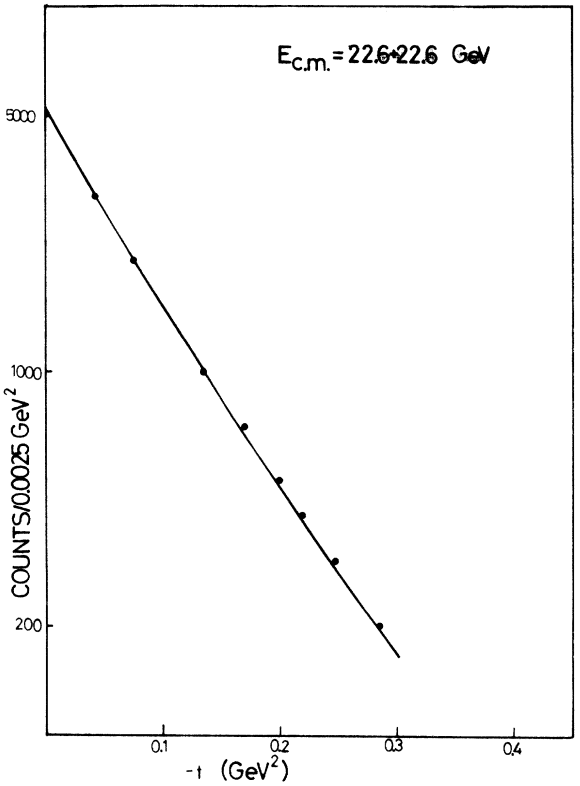

FIG. 2. Equation (4) compared with some typical points from Ref. 5, with normalization to give agreement at $t = 0$.

the photon couples, displaying explicitly the quark charges[10]:

$$W_i = \tfrac{4}{9}(W_i^{\mathcal{P}\mathcal{P}} - W_i^{\mathcal{P}\mathfrak{N}} - W_i^{\mathcal{P}\lambda}) + \tfrac{1}{9}(W_i^{\mathfrak{N}\mathfrak{N}} + W_i^{\lambda\lambda} + 2W_i^{\mathfrak{N}\lambda}), \quad i = 1, 2 . \tag{9}$$

For example, $W_i^{\mathcal{P}\mathcal{P}}$ refers to the contribution from $\mathcal{P}$ quarks, and $W_i^{\mathcal{P}\mathfrak{N}}$ represents the interference between the contributions from $\mathcal{P}$ and $\mathfrak{N}$ quarks. (The interference terms are negligible at large q^2.) We obtain, at high energy and small t,

TABLE I. Comparison between $d\sigma/dt$ given by Eq. (4) and experiment.

s (GeV^2)	Average $\lvert t\rvert$ (GeV^2)	Range of $\lvert t\rvert$ (GeV^2)	Slope parameter (experimental) (GeV^2)	Slope parameter predicted (Pom. slope: 0.25) (GeV^2)
462	0.072	0.050–0.094	11.57 ± 0.03	11.45
	0.188	0.138–0.238	10.42 ± 0.17	10.30
949	0.068	0.046–0.090	11.87 ± 0.28	11.86
	0.189	0.138–0.240	10.91 ± 0.22	10.65
2013	0.0675	0.046–0.089	12.87 ± 0.20	12.23
	0.1875	0.136–0.239	10.83 ± 0.20	11.04
2808	0.086	0.060–0.112	12.40 ± 0.30	12.19
	0.238	0.168–0.308	10.80 ± 0.20	10.79

$$\frac{d^2\sigma}{dtdM^2} \sim \frac{9\beta^4[F_1^p(t)]^2}{4\pi \sin^2[\frac{1}{2}\pi\alpha_P(t)]} \left(\frac{s}{M^2}\right)^{2\alpha_P(t)-2} \times \left[\frac{\tilde{W}_2}{2m}\left(1-\frac{M^2}{s}\right) - \frac{m\tilde{W}_1}{s^2}(t+2m^2)\right] , \tag{10}$$

where

$$\tilde{W}_i = W_i^{\mathcal{P}\mathcal{P}} + W_i^{\mathfrak{N}\mathfrak{N}} + W_i^{\lambda\lambda} + 2W_i^{\mathcal{P}\mathfrak{N}} + 2W_i^{\mathcal{P}\lambda} + 2W_i^{\mathfrak{N}\lambda} . \tag{11}$$

Except at very small t, the $\tilde{W}_1$ term in (10) is negligible compared with the $\tilde{W}_2$ term, being multiplied by a factor s^{-2}. For large M^2, $\tilde{W}_2$ is dominated by Reggeon exchange:

$$\tilde{W}_2 \sim g_P(t)(M^2)^{\alpha_P(0)-2} + g_R(t)(M^2)^{\alpha_R(0)-2} , \tag{12}$$

where α_R is the vector-meson trajectory. Thus (10) contains contributions from triple-Regge vertices[11] of both PPP and PPR types. Our inclusion of the factor $(M^2)^{2-2\alpha_P(t)}$ in (10) gives these contributions the correct[12] dependence on s and M^2. Gauge invariance in electroproduction requires $\tilde{W}_2$ to vanish at $t=0$, so that in this model the leading contributions from the PPP and PPR vertices vanish at $t=0$ and there is a dip in the diffractive processes at small t. At very small t the $\tilde{W}_1$ term in (10) becomes relatively important: For small q^2 gauge invariance for electroproduction results in

$$\tilde{W}_1 \approx \frac{\nu^2}{q^2}\tilde{W}_2 . \tag{13}$$

In electroproduction, for $M \gtrsim 2.5$ GeV and $q^2 \gtrsim 1$ GeV^2 there is Bjorken scaling:

$$\nu W_2(\nu, q^2) \sim F_2(\omega), \quad \omega = 2m\nu/q^2 . \tag{14}$$

For smaller values of q^2, and $\omega \gtrsim 5$, it seems a fair approximation to take[13]

$$\nu W_2(\nu, q^2) = \phi(q^2)F_2(\tilde{\omega}) , \quad \phi(q^2) = \frac{q^2}{q^2+a^2} , \quad \tilde{\omega} = \frac{2m\nu}{q^2+b^2} . \tag{15}$$

For lack of further information, we assume that each of the functions W_2^{rs} on the right of (9) approaches Bjorken scaling in the same way:

$$\nu W_2^{rs}(\nu, q^2) = \phi(q^2)F_2^{rs}(\tilde{\omega}) , \tag{16}$$

where $F_2^{rs}(\omega)$ is the Bjorken limit of νW_2^{rs}. In the simple quark-parton model,[1]

$$F_2^{\mathcal{P}\mathcal{P}}(\omega) = 2V(\omega) + 2S(\omega) , \quad F_2^{\mathfrak{N}\mathfrak{N}}(\omega) = V(\omega) + 2S(\omega) , \quad F_2^{\lambda\lambda}(\omega) = 2S(\omega) , \quad F_2^{rs}(\omega) = 0 , \ r \neq s \tag{17}$$

where the function $V(\omega)$ corresponds to valence-quark contributions and $S(\omega)$ represents contributions from the sea. Thus

$$F_2(\omega) = V(\omega) + \tfrac{4}{3}S(\omega) \tag{18}$$

and

$$\nu\tilde{W}_2 = \phi(q^2)[3V(\tilde{\omega}) + 6S(\tilde{\omega})] . \tag{19}$$

At large ω, the function S is dominated by Pomeron exchange and the function V by meson exchange. At $\omega = 20$, $V \approx 2S$, and so from (19) the

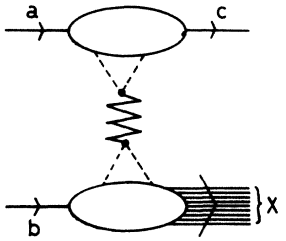

FIG. 3. Diagram for $pp \to pX$.

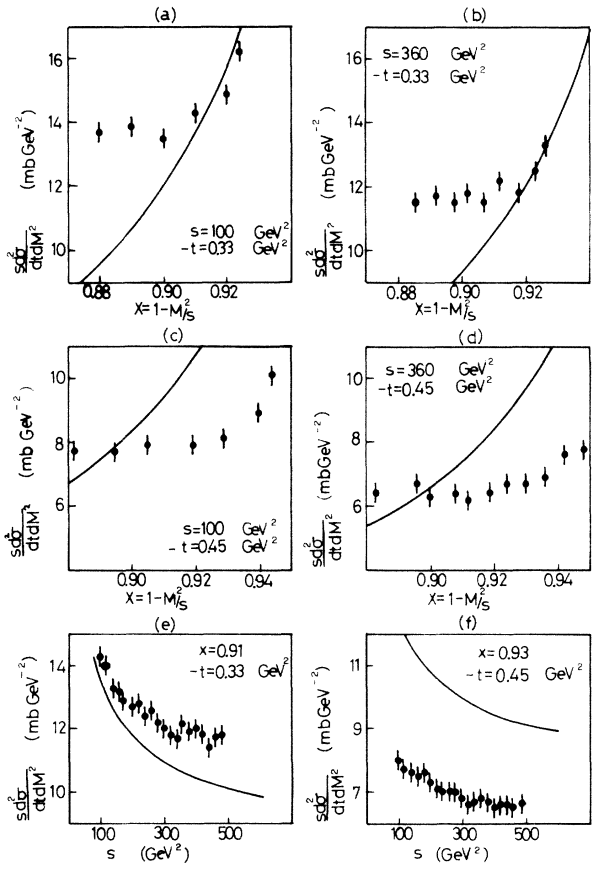

FIG. 4. Equation (22) compared with data from Sannes *et al.* (Ref. 6).

implication is that at $M^2/|t| \approx 20$ the PPP and PPR contributions to $pp \to pX$ are roughly equal. We estimate that at $M^2/|t| = 100$ the PPR contribution is still about half of the PPP, though there is uncertainity about the magnitude of $S(\omega)$ for very large ω. In our calculations, we shall use the approximate forms[1]

$$V(\omega) = \frac{15}{16}\frac{(1-\omega^{-1})^2}{\sqrt{\omega}}\,, \qquad S(\omega) = \tfrac{1}{10}(1-2/\omega)\,, \quad \omega > 2\,. \tag{20}$$

The parameters a and b in (15) are then determined by the requirement that at $q^2 = 0$, $4\pi^2\alpha\nu W_2/q^2$ is equal to the total cross section for photoabsorption. For the latter we use the phenomenological high-energy fit[14] $\sigma_\gamma = 98.7 + 64.9E_\gamma^{-1/2}$ and then with (18) and (20) we obtain

$$a^2 = 0.15\ \text{GeV}^2, \quad b^2 = 0.015\ \text{GeV}^2\,. \tag{21}$$

Our final expression is

$$\frac{d^2\sigma}{dtdM^2} = \frac{9\beta^4[F_1^p(t)]^2}{4\pi\sin^2[\frac{1}{2}\pi\alpha_P(t)]}\,\frac{\phi(-t)[3V(\bar\omega)+6S(\bar\omega)]}{\omega|t|} \times\left(\frac{s}{M^2}\right)^{2\alpha_P(t)-2}\left(1-\frac{M^2}{s}+\frac{m^2M^4}{s^2t}\right)\,, \tag{22}$$

with β given in (5), $F_1^p(t)$ in (6), $\alpha_P(t)$ in (7), ϕ in (15) and (21), and the functions V and S in (20). Because b^2 in (21) turns out to be so small, except at very small t one can put

$$\bar\omega \approx \omega = \frac{M^2 - m^2 - t}{2|t|}\,. \tag{23}$$

In Figs. 4 and 5 we give some representative plots of (22), together with published data.[6] For a model that has no adjustable parameters, and which is not expected to have more than approximate validity, the agreement with the data in both normalization and general shape is surprisingly good.

One of us (P.V.L.) is grateful to Dr. L.-L. Wang for a valuable discussion. The other (G.J.) is grateful to the Science Research Council for a grant.

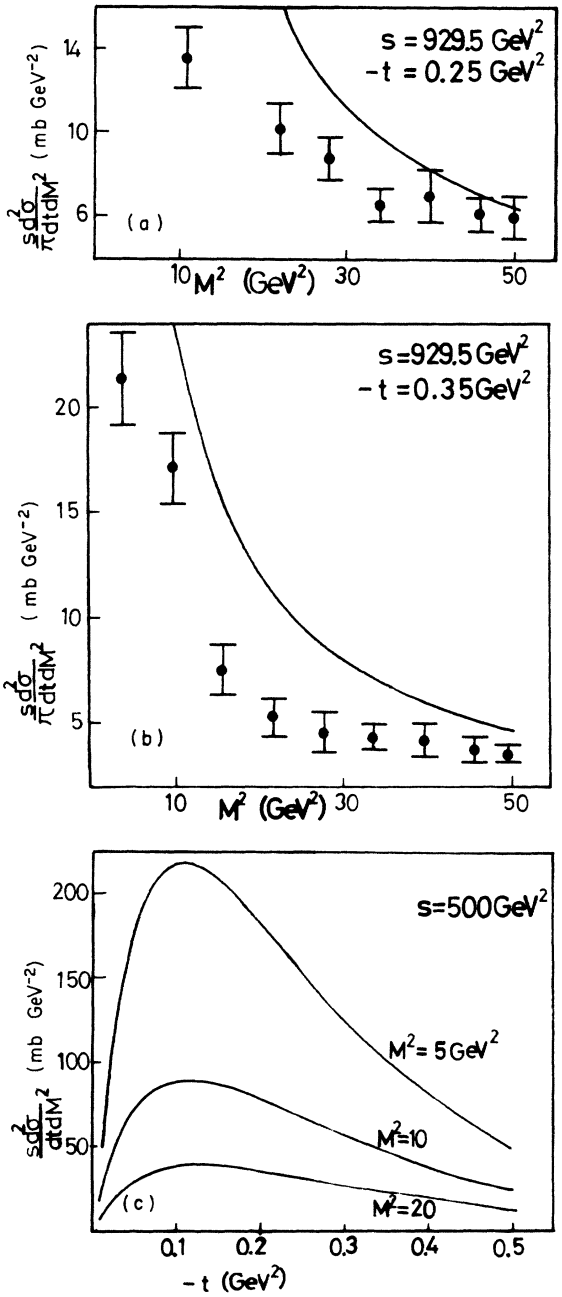

FIG. 5. (a) and (b) Equation (22) compared with data from Albrow *et al.* (Ref. 6). (c) Predicted $sd^2\sigma/dtdM^2$ versus M^2 at fixed t.

[1] P. V. Landshoff and J. C. Polkinghorne, Nucl. Phys. B28, 240 (1971); Phys. Lett. 34B, 7, 621 (1971); J. Kuti and V. F. Weisskopf, Phys. Rev. D 4, 3418 (1971). A recent review is given by P. V. Landshoff, Rutherford High-Energy Laboratory Report No. RL-73-018 (unpublished).

[2] P. V. Landshoff and J. C. Polkinghorne, Nucl. Phys. B32, 541 (1971).

[3] A closely related approach is that of F. Ravndal, Phys. Lett. 37B, 300 (1971).

[4] V. Amaldi *et al.*, Phys. Lett. 43B, 231 (1973).

[5] G. Barbiellini *et al.*, Phys. Lett. 39B, 663 (1972).

[6]F. Sannes *et al.*, Phys. Rev. Lett. 30, 766 (1973); M. G. Albrow *et al.*, Nucl. Phys. B54, 6 (1973).
[7]S. Berman and M. Jacob, Phys. Rev. Lett. 25, 1683 (1970).
[8]P. V. Landshoff and J. C. Polkinghorne, Ref. 1 and Phys. Rep. 5C, 1 (1972), especially section 2.4.
[9]H. Kendall, in *Proceedings of the 1971 International Symposium on Electron and Photon Interactions at High Energies*, edited by N. B. Mistry (Laboratory of Nuclear Studies, Cornell Univ., Ithaca, N.Y., 1972).
[10]Because of its quantum numbers, the photon couples only to valence quarks in the elastic amplitude, but in the inelastic amplitude the sea also contributes. In Ref. 2 special arguments were given to show why the Pomeron might emulate the photon, in spite of its different quantum numbers.
[11]P. V. Landshoff and W. J. Zakrzewski, Nucl. Phys. B12, 216 (1969).
[12]C. E. DeTar, C. E. Jones, C.-I Tan, F. E. Low, J. H. Weis, and J. E. Young, Phys. Rev. Lett. 26, 675 (1971).
[13]Kendall, Ref. 9, Fig. 2. See also F. Close and J. Gunion, Phys. Rev. D 4, 742 (1971).
[14]G. Wolf, in *Proceedings of the 1971 International Symposium on Electron and Photon Interactions at High Energies*, edited by N. B. Mistry (Ref. 9).